SUBTHRESHOLD PHOTONS IN HEAVY-ION COLLISIONS*

Y. Schutz

for the TAPS Collaboration**

Grand Accélérateur National d'Ions Lourds
BP 5027, F-14021 Caen, France

(Received December 8, 1995)

Subthreshold bremsstrahlung photons are shown to be a unique probe of nuclear matter when it is in a well defined thermodynamical phase during a heavy-ion collision. From their emission pattern which closely follows the nuclear reaction dynamics we deduced a new interpretation of the two-photon correlation function. We also show that very energetic photons are produced but their origin cannot solely be explained by the bremsstrahlung process and the known hadronic contributions.

PACS numbers: 25.20.Dc

1. Introduction

I was tempted to subtitle this lecture *Hard Photons II: the return* since it will be the continuation of two lectures given two years ago at the *XXIII Mazurian Lakes Summer School.* In these lectures two problems were raised and remained unsolved. The first problem [1] appeared with our measurement of the two-photon correlation function in which we have identified the expected interference effect. We were however unable to understand why the deduced source size came out to be larger than the size of the colliding heavy-ion system! The second problem was raised by Matulewicz [2]. He showed a photon spectrum measured at 60 *A*MeV projectile energy which

---

* Presented at the XXIV Mazurian Lakes School of Physics, Piaski, Poland, August 23–September 2, 1995.

** The TAPS Collaboration is a joint venture between GANIL (France), University of Gießen (Germany), GSI (Germany), KVI (The Netherlands), NPI (Czech Republic) and University of Valencia (Spain).

extends up to 300 MeV that is five times the beam energy per nucleon, this high energy limit being imposed only by the limit of sensitivity of our experimental conditions. It was also the first time that such energetic photons were measured in a heavy-ion collision at comparatively low bombarding energy. The problem was then to understand how in a heavy-ion collision this amount of energy can be concentrated on a single degree of freedom.

Since TAPS is a travelling detector which offers the exciting opportunity to cover a very broad scientific program [3], we could not repeat in the last two years the experiments and collect more information which could have helped to solve our problems. Instead we analyzed our old data again adopting a different point of view, largely suggested by predictions on the dynamics of the nuclear reaction obtained from model calculations. This approach turned out to be very fruitful since we are now able to propose a solution to our first problem and we have made some progress toward a solution to our second problem. However we have not yet achieved to interpret the whole measured photon spectrum. How we reached our goal and what is the present status of our understanding will be the subject of the present lecture. I will start with a long introduction which will help to situate the study of the photon emission in the more general context of heavy-ion physics.

2. Probing the reaction dynamics with hard photons

To translate the macroscopic behaviour of nuclear matter in terms of an equation of state (EOS) stands as one of the most challenging objective in modern nuclear physics. So far we know with a good accuracy only its properties at zero temperature and pressure, *i.e.*, the saturation density and the binding energy of nuclei. We have a rather vague idea on the value of the incompressibility modulus which ranges between 200 and 400 MeV [4]. A way to extend our knowledge consists in studying the response of nuclear matter to heat and pressure as it can be done by colliding heavy ions at various bombarding energies. The drawback of such a study is that heavy-ion collisions allow to form hot and dense nuclear matter only during very short times and rather provide a dynamical exploration of the phase diagram. As a consequence any observable will convey information on both the dynamics of the collision and the physics of interest for the EOS. The experimental challenge is thus to disentangle these two pieces of information. This can be partly achieved by a proper choice of the observable. Presently most popular candidates are the collective flow of nucleons or particles created during the nuclear reaction (see the lecture by Hildenbrand) which probes the dissipation of kinetic energy into compression energy, or the multi-fragmentation of the di-nuclear system (see the lecture by Plagnol) which probes the dissipation of kinetic energy into heat. Of course information on the EOS cannot be read directly from the data but one must rely on model calculations which treat the reaction dynamics at the best of our present knowledge. The problem arises from several uncontrolled parameters. In the models they can lead to similar effects on the observables as the effects expected from the properties of the EOS, for example the value of the incompressibility modulus [5].

As an alternative and complementary probe we suggest to select bremsstrahlung photons. They have the unique property to be emitted at well defined instants of the collision and only during very short periods as compared to the collision time. Their source thus corresponds also to a well defined thermodynamical state and their emission pattern reflects the properties of this state. Moreover, since photons only experience weak electromagnetic final state interactions they provide us with an unperturbed image of their source. Let us know examine what the properties of the hard-photon emission are and what model calculations predict about the production of bremsstrahlung photons.

2.1. Properties of the hard-photon emission in heavy-ion collisions

In the photon spectrum hard photons are conventionally defined as those with an energy above the energy of the Giant Dipole Resonance. The many measurements performed in the last 10 years [6, 7] on the hard-photon emission in heavy-ion collisions were interpreted by attributing the origin of hard photons to the incoherent superposition of bremsstrahlung emitted in individual proton-neutron (pn) collisions. From their spatial emission pattern it was further concluded that they are mainly emitted in first chance pn collisions so that the main photon source is localised at the very beginning of the nuclear reaction.

The bremsstrahlung spectrum emitted in a free pn collision as calculated within the frame of classical electrodynamics follows an $1/E_\gamma$ energy dependence. The high energy cutoff of the spectrum is deduced from the energy $\sqrt{s}$ available in the centre-of-mass:

$$E_\gamma^{\max} = \frac{s - 4m_N^2}{2\sqrt{s}}, \qquad (1)$$

where m_N is the nucleon mass. This energy amounts approximately to half the beam energy. In a heavy-ion collision the centre-of-mass energy available in an in-medium pn collision is increased by the intrinsic momentum of nucleons due to the Fermi motion which adds to the relative projectile momentum. The consequence on the photon production, of this extra energy

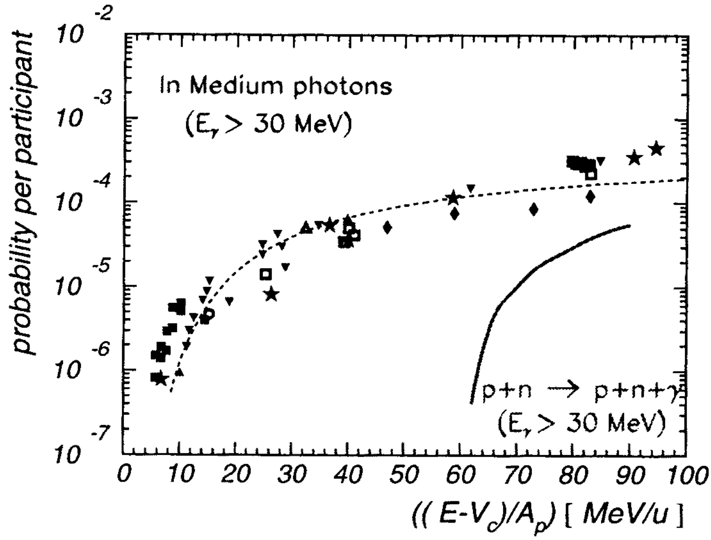

Fig. 1. Production probability of bremsstrahlung photons ($E_\gamma \geq 30$ MeV) calculated for free proton-neutron collisions (solid line) as a function of the bombarding energy corrected for the Coulomb barrier. The discrete symbols represent the same probability measured in heavy-ion collisions and scaled by the average number of participants. The dashed line is a fit to the data.

made available to the pn collision is illustrated in figure 1. Photons with energies larger than 30 MeV are considered. The bremsstrahlung emission probability calculated [8] for free pn collisions as a function of bombarding energy corrected for the Coulomb barrier is displayed as the solid line. The threshold given by equation (1) is evidenced at $\approx$ 60 MeV. The same dependence of the probability measured in heavy-ion collisions and scaled by the number of participants [7, 9] is represented on the figure by the various symbols. It represents the photon production in an in-medium pn collision. The huge difference between free and in-medium production pinpoints the role played by the Fermi motion of participant nucleons. It extends the photon production well below the threshold and allows for the emission of subthreshold photons defined by:

$$E_\gamma^{\text{subthreshold}} > \frac{1}{2} \frac{E_{\text{beam}}}{\text{nucleon}} . \tag{2}$$

Subthreshold photons are of a very particular interest in our study of the thermodynamical properties of nuclear matter since their energy spectrum only reflects the phase-space occupancy of nucleons within the interaction zone. We thus have at hand a direct mean to measure thermodynamical quantities like the density and temperature of the participant zone at the very precise instants when these photons are emitted.

From there on we need to be guided by model calculations to have a better determination of the time scale of the photon emission.

2.2. BUU predictions for the bremsstrahlung-photon emission

A model of heavy-ion collisions at energies per nucleon around the Fermi energy ($E_{\rm F} \approx 40$ MeV) must describe the collision between nucleons while they are moving through a mean-field potential. This is done by solving the Boltzmann transport equation (see the lecture by Randrup) which takes the general form:

$$\frac{d}{dt} f(\vec{r}, \vec{p}, t) = I\left[f(\vec{r}, \vec{p}, t)\right] . \tag{3}$$

It describes the time evolution of the one-body density distribution $f(\vec{r}, \vec{p}, t)$, *i.e.*, the probability to find at time t a nucleon with momentum $\vec{p}$ at location $\vec{r}$. The right-hand side of equation (2), the collision integral, describes the collision between nucleons. Several models have been developed which all share the common feature of using the pseudo-particle idea [4] to simulate the physics of the semi-classical transport equation (3). Some quantum mechanics are implemented in the equation to take into account the Pauli exclusion principle during the nucleon-nucleon (NN) scattering.

Owing to the very low probability to produce a bremsstrahlung photon ($P_\gamma \approx 10^{-3}$ per participant at $100A$ MeV bombarding energy) photons can be treated pertubatively, *i.e.*, they will not participate to the reaction dynamics. The elementary cross section of the process $n + p \rightarrow n + p + \gamma$ is calculated using the T-matrix formalism [7, 8]. The total flux of photons is obtained by summing incoherently photons from all the pn collision:

$$\frac{dN_\gamma}{dE_\gamma} = 2\pi \int b db \sum_{NN} \int \frac{d\Omega'}{4\pi} \frac{E_\gamma}{E'_\gamma} \frac{dP_\gamma^{NN}(\sqrt{s})}{dk'} \bar{f}_2 \bar{f}_3 , \tag{4}$$

where E_γ is the photon energy Doppler shifted to the frame moving with the NN centre-of-mass velocity, the factor E_γ / E'_γ the jacobian of the Lorentz transformation, and Ω' the phase space available in the final state of the collision $\vec{p} + \vec{p}_1 \rightarrow \vec{p}_2 + \vec{p}_3 + \vec{p}_\gamma$ weighted by the Pauli blocking factor $\bar{f}_2 \bar{f}_3$. The average over the impact parameter b is finally performed.

Let us now first examine the predictions made by the Boltzmann-Uehling-Uhlenbeck (BUU) code developed by the theory group of the University of Gießen [7, 10]. We can distinguish two kinds of scenario depending on the bombarding energy. For a symmetric system and a central collision, at bombarding energies above 50 AMeV the two colliding nuclei overlap to form a dense di-nuclear system. Immediately after the system expands violently and breaks into fragments. At bombarding energies below 50 AMeV a dense di-nuclear system is again formed in the early stage of the collision. However, now the system expands slowly up to the point where the attractive part of the nuclear force is strong enough to drive a second compression. The di-nuclear system subsequently undergoes a density oscillation around the saturation density and ultimately may fuse partially to form a hot nucleus. Such a scenario is illustrated in figure 2. where the time evolution of the pseudo-particle density is represented in coordinate space. In figure 3. the same nuclear reaction is represented in momentum space. At the beginning of the collision, during the first compression the two Fermi spheres are separated by the relative momentum of the projectile. However already during the second compression we observe that the momentum distribution is isotropic, *i.e.*, the di-nuclear system is thermalised.

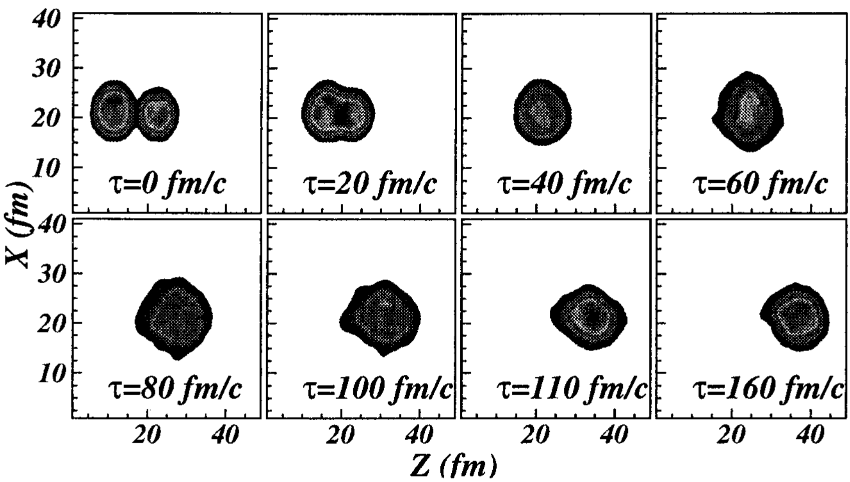

Fig. 2. Time evolution of the reaction Kr + Ni at 30 *A*MeV shown as the density distribution of test particles projected in the *XZ* coordinate space. The beam axis is along the *Z* direction.

The bremsstrahlung-photon emission (figure 4.) follows closely the reaction dynamics depicted previously. Their calculated emission rate is plotted as a function of the collision time for three different bombarding energies and three different photon energies. At the lowest bombarding energies, besides the dominant photon emission from first chance pn collisions a second less intense source is evidenced. It coincides with the second compression. For the highest bombarding energy since the density oscillation does not show up, photons are emitted only at the beginning of the reaction. The picture is then the following. A first flash of photons is produced in the first stage of the collision when the di-nuclear system has reached the high-

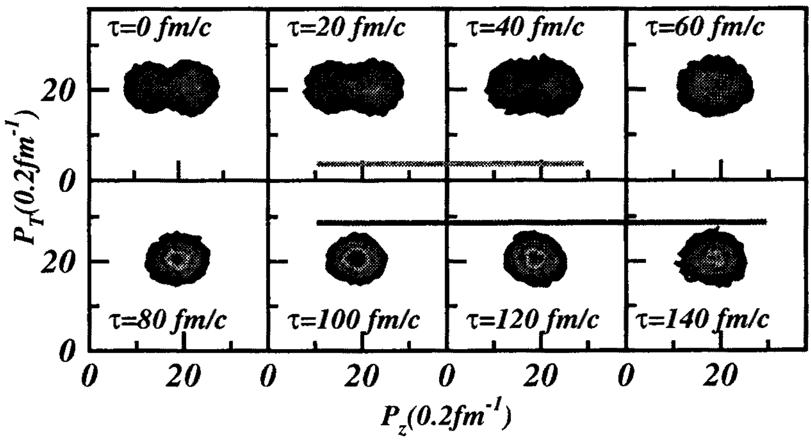

Fig. 3. Time evolution of the reaction Kr + Ni at 30 AMeV shown as the density distribution of test particles projected in the $P_Z P_\perp$ momentum space. The beam momentum is along P_Z.

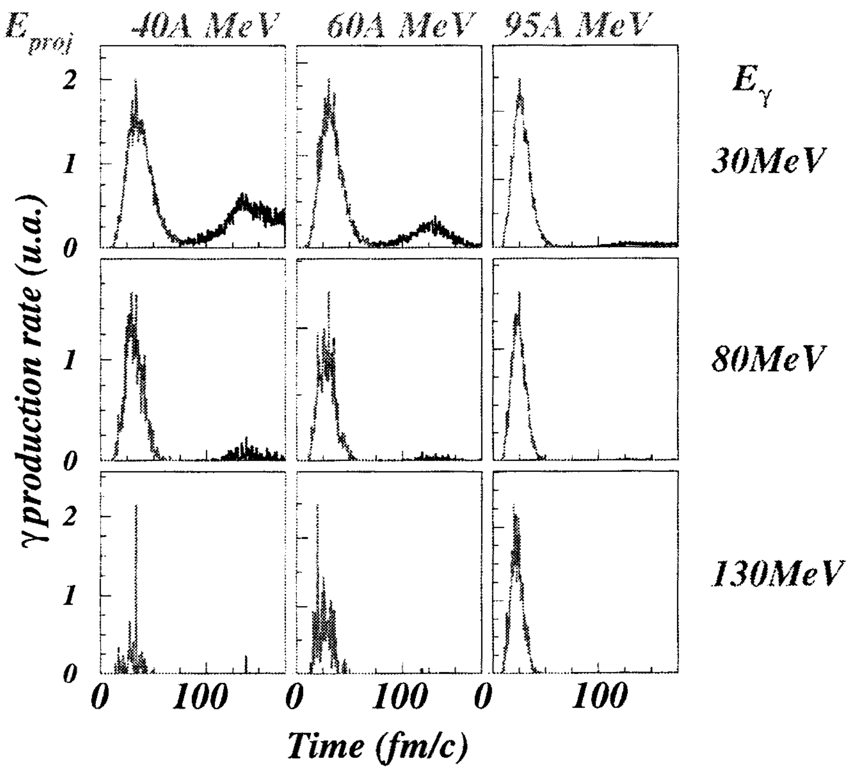

Fig. 4. Bremsstrahlung-photon production rate calculated with BUU in the reaction Kr + Ni for three bombarding energies and for three photon energies as a function of the collision time.

est density. We call these photons *direct* photons. They will be exploited to probe cold and dense nuclear matter. Later in the reaction a second flash of photons arises, when the bombarding energy is moderate enough, as a result of subsequent pn collisions. These photons are emitted from a thermalised system and we therefore call them *thermal* photons. They will be exploited to probe hot nuclear matter. We thus have at hand a probe which carries information on two distinct and thermodynamically well defined phases of nuclear matter for which we can now determine quantities like the density, the temperature and the incompressibility modulus. In an analysis which I have no time here to describe we found that in the reaction Kr + Ni at 60 *A*MeV the system can be compressed up to a density 40% above the saturation density [11, 12], and heated to temperatures as high as 8 MeV [13, 14]. We finally deduced a value for the incompressibility modulus $K_\infty = 290 \pm 50$ MeV.

Let us now examine the consequences of the photon emission dynamics on the interference pattern.

3. New interpretation of the two-photon correlation function

The theory of the interference between two identical particles also known as Hanbury–Brown and Twiss effect, or Bose–Einstein correlation will be given in details during the lecture by Cindro or can be found in the proceedings of the previous Summer School [1]. Let me just summarise by recalling that two identical particles emitted from a chaotic source localised in space and time give rise to an interference pattern which can be evidence in the two-particle correlation function at small relative four-momentum. The shape of the pattern is an image of the Fourier transform of the source density distribution. The correlation function is constructed as the ratio of the two-particle coincidence yield and an uncorrelated background generated by folding the single photon yields. Assuming a Gaussian distribution for the density distribution the correlation function exhibits a Gaussian-like pattern from which the source size can be extracted. This is exactly what we have done with our data measured for the two systems Kr + Ni at 60 *A*Mev and Ta+Au at 40 *A*MeV. And as said at the beginning of this lecture we found to our surprise a much too large source size [1, 15].

If we now take into account the prediction of the calculations shown in the previous section and consider the existence of two sources of photons we must rewrite the density distribution in the space-time coordinates $r = (\vec{r}, t)$ as:

$$\sqrt{I_\mathrm{d}}\rho(r) + \sqrt{I_\mathrm{t}}\rho(r + \Delta r)\,, \qquad (5)$$

where I_d and I_t are the relative intensities of the *direct* and *thermal* photon sources respectively and Δr the space-time separation of the two sources.

The corresponding correlation function is then deduced from the Fourier transform of equation (5) [15, 16]:

$$C_{12} = 1 + \lambda \exp\left(\frac{Q^2 R^2}{2\hbar^2 c^2}\right) \times \mathcal{I}(Q)\ , \tag{6}$$

$$\mathcal{I}(Q) = I_{\rm d} + I_{\rm t} + 2\sqrt{I_{\rm d} I_{\rm t}} \cos\left(\frac{Q\Delta r'}{\hbar c}\right). \tag{7}$$

Equation (6) is the projection of the four-dimensional correlation function on Q, the relative four-momentum which for photons is also the invariant mass, and λ is a fit parameter. The choice of this specific representation has a double motivation. First the limited statistics do not permit a multi-dimensional representation. Second the invariant mass representation allows to localise the important contribution of the two-photon decay of the neutral pion in a region where photons are not correlated. However, although equation (6) will provide with a good description of the data its derivation is not exact. Therefore the parameters R and $\Delta r'$ are not a direct measurement of the space-time extent and separation of the sources [16]. In equation (6) the difference from the one source hypothesis lies in the *interference* factor of equation (7) which modulates the Fourier transformation of the source distribution. It depends only on the relative intensity of the two sources and on a parameter which is related to the spatial and temporal separation of the sources.

In figure 5. the experimental correlation function is compared to equation (6). On the left-hand side the one measured for the system Kr + Ni at 60 *A*MeV. The data are well described by a source size of 3.3 ± 0.9 fm which translates into a root-mean-square radius of 5.7 ± 1.6 fm and a *thermal*-photon source intensity of 30% of the total hard photon intensity. On the right-hand side of figure 5. is shown the correlation function for the system Ta+Au at 40 *A*MeV. Because, as found in the energy spectrum [11], the two sources have now equal intensities, the amplitude of the oscillations given by equation (7) are maximum. Since the bombarding energy is also lower than in the previous system, the separation between the two sources should also be different, hence the frequency of the oscillations should be different. That is exactly what is observed in the data. They are best described by a source size of 4.5 ± 1.5 fm or a root-mean-square radius of 7.8 ± 2.6 fm.

This solves our first puzzle.

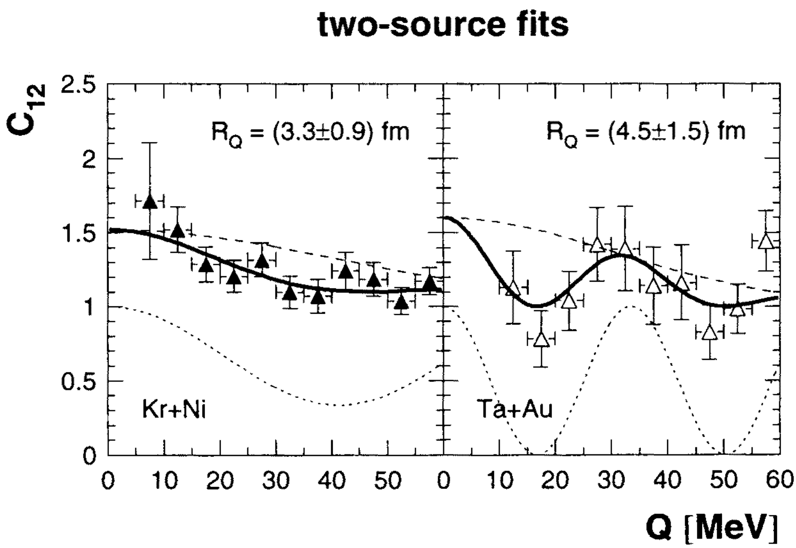

Fig. 5. Correlation functions measured for the systems Kr+Ni at 60 *A*MeV (left-hand spectrum) and Ta + Au at 40 *A*MeV (right-hand spectrum) as a function of the invariant mass Q. The solid line represents equation (6), the dashed line represents equation (7), and the dotted line the ratio of the two.

4. The high-energy part of the photon spectrum

In figure 6. we have displayed the photon spectrum measured in the reaction Kr + Ni at 60 *A*MeV. At the low energy end of the spectrum one recognises the exponential decay of the statistical emission of photons from hot fragments. Above 30 MeV according to our definition (equation (2)) we localise the subthreshold bremsstrahlung photons which show up as two exponential distributions. The softer one (below $E_\gamma = 50$ MeV) is associated to the *thermal* photons and the harder one to the *direct* ones. This identification is justified by the results of the calculations displayed in figure 4. It is a consequence of the thermalisation of the system during which much of the initial energy is dissipated as heat. Therefore the energy available in the pn centre-of-mass is on the average smaller when *thermal* photons are emitted than at the beginning of the nuclear reaction.

The maximum photon energy one can expect in a single in-medium pn collision can be calculated from equation (1) considering that the two intrinsic momenta are in opposite direction, parallel to the beam momentum, and with a maximum absolute value given by the saturation density. We find $E_\gamma^{\max} = 180$ MeV. We observe in figure 6. that this limit is noticeably surpassed and photons with energies even up to 300 MeV could be measured.

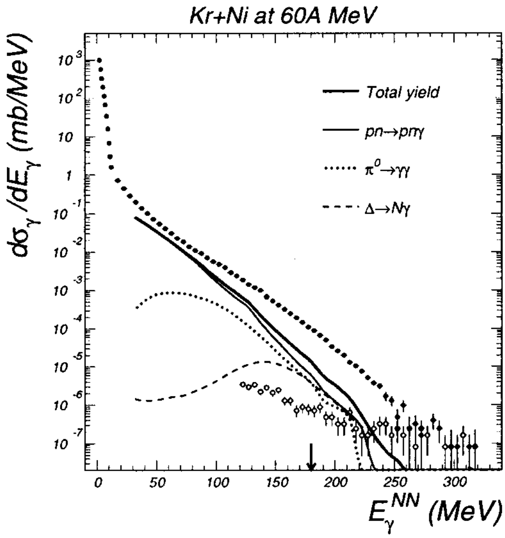

Fig. 6. Photon-energy spectrum (closed circles) obtained from the measured photon spectrum after subtraction of the various contributions also displayed in the figure. The open circles represent the cosmic contribution measured during off-beam periods and which passed our identification algorithm. The reaction is Kr + Ni at 60 *A*MeV. The arrow indicates the maximum photon energy calculated from equation (2).

The highest limit of the present spectrum is only imposed by the sensitivity of the experiment which was of the order of one nb. With such low cross-sections cosmic events detected in random coincidences and not fully identified by our photon identification algorithm [17] compete with photons from the nuclear reaction. This cosmic-events contribution was measured during the experiment and already subtracted from the photon spectrum (figure 6.).

It is not too much of a surprise that the photon spectrum extends above 180 MeV since this limit was calculated fixing the intrinsic momentum equal to the value given by a sharp-cutoff Fermi distribution. In doing so we ignore for example the high momentum components evidenced in electron scattering [18], but, may be more important, we neglect the dynamical changes the momentum distribution surely undergoes during the collision. A signal for strong dynamical modifications may be seen in the changes of the photon spectrum slope so that photons are produced with harder spectra in central collisions than in peripheral ones [19]. Several mechanisms responsible for such modifications can be invoked like three body collisions which become important at high densities [5], dynamical fluctuations which may accumulate energy in one single pn collision [20], or processes involving secondary particles such as pions or Δ resonances which act as energy storage. Although there does not yet exist an unique description which takes into account all quantum effects (off-shell effects for nucleons are for example not present in the classical transport equation) and all the mechanisms mentioned earlier, a rough estimate of the magnitude of their effects on the photon spectrum has demonstrated that none of these processes alone can account for all the measured photons above the maximum energy.

So far we have however ignored the pion in-medium dynamics. Pions are produced [16] at 60 AMeV with cross sections comparable to photons with energies $E_\gamma = m_\pi c^2 + T_\pi$ where T_π is the pion kinetic energy. The most obvious contribution to the photon spectrum comes from the two-photon decay of the neutral pions. This contribution was measured in our experiment, it is plotted on figure 6. We observe that through the whole spectrum this contribution remains below the calculated pn bremsstrahlung spectrum. Since pions can be produced via the Δ resonance in inelastic NN scattering we must also consider the photon decay of the Δ which has a branching ratio of 0.006. This contribution was calculated by considering that the Δ isobars are formed so that the effective mass of the πN system follows the Δ mass distribution, its width depending on the pion momentum in the centre-of-mass. We finally assumed that all the measured pions are produced through a Δ. The resulting photon spectrum was folded with the TAPS acceptance and response function and has passed our analysis algorithm. It is displayed in figure 6. This contribution remains negligible until an energy of approximately 150 MeV where it becomes comparable to the contribution of the bremsstrahlung photons. Adding all the three contributions together, pn bremsstrahlung, neutral pion decay and Δ decay, leaves us with a spectrum which by far underpredicts the experimental one.

We therefore have not yet solved our second puzzle. However we have still to consider possible sources of photons which might result from the pion final-state interactions in the nuclear medium. This work is in progress.

5. Conclusion

It is possible in a two year period to give two different lectures on a same subject, using the same set of data but with rather different results. The secret resides in the fact that we could devote enough time to the data analysis and that we were not bothered by new data tapes piling up on our shelves. Guided by the predictions of the transport equation for the collision dynamics and its influence on the bremsstrahlung photon emission we interpreted the two-photon correlation function in a rather different way. We assumed that photons are emitted from two distinct sources shining at two different times of the reaction and with relative intensities only governed by the reaction dynamics. This assumption lead us to a very satisfactory description of the two measured correlation functions qualitatively as well as quantitatively since we deduced source sizes which now make more sense.

We achieved also some progress in the understanding of the high energy part of the measured photon spectrum. Having considered several potential photon sources, pn bremsstrahlung, neutral pion decay and Δ-resonance decay, we are left with photons the origin of which remains unexplained. The clue might come from the pion final state dynamics which could generate the very energetic photons we have measured. This could be the introduction to a new lecture at the next *Mazurian Lakes Summer School.*

The TAPS data presented here result from a group effort. The contributions of F.M. Marqués, G. Martínez, T. Matulewicz, R.W. Ostendorf, P. Lautridou, F. Lefèvre, W. Mittig, P. Roussel-Chomaz, J. Québert, J. Díaz, A. Marín, R. Holzmann, S. Hlávač, A. Schubert, R. Simon, V. Wagner, H. Löhner, J.H.G. van Pol, R.H. Siemssen, H.W. Wilschut, M. Franke, and Z. Sujkowski as well as many discussions with H. Delagrange, M. Płoszajczak, and Gy. Wolf are gratefully aknowledged. In particular, I would like to thank F.M. Marqués, G. Martínez and T. Matulewicz who carried the major load of data analysis and performed the calculations. The data were taken at the GANIL accelerator facility in Caen, France. This program is supported by IN2P3 and CEA (France), BMFT (Germany), FOM (The Netherlands), and CICYT (Spain).

REFERENCES

[1] Y. Schutz, *Acta Phys. Pol.* **B25**, 485 (1994).
[2] T. Matulewicz, *Acta Phys. Pol.* **B25**, 705 (1994).
[3] H. Ströher, to be published in *Nucl. Phys. News Int.*, (1995).
[4] Z. Sujkowski, *Physica Scr. T* **56**, 320 (1995).
[5] A. Bonasera *et al.*, *Phys. Rep.* **243**, 1 (1994).
[6] H. Nifenecker, J.A. Pinston, *Prog. Part. Nucl. Phys.* **23**, 271 (1989).
[7] W. Cassing *et al.*, *Phys. Rep.* **188**, 364 (1990).
[8] M. Schäfer *et al.*, *Z. Phys.* **A339**, 391 (1991).
[9] H. Nifenecker, J.P. Bondorf, *Nucl. Phys.* **A442**, 478 (1985).
[10] Gy. Wolf *et al.*, *Nucl. Phys.* **A517**, 517 (1990); Gy. Wolf *et al.*, *Nucl. Phys.* **A552**, 549 (1993).
[11] G. Martínez *et al.*, *Phys. Lett.* **B349**, 23 (1994).
[12] G. Martínez, Thèse Université de Valencia (Spain), GANIL T94-06.
[13] D. Neuhauser, S.E. Koonin, *Nucl. Phys.* **A462**, 163 (1987).
[14] G. Martínez *et al.*, to be published.
[15] F.M. Marqués *et al.*, *Phys. Rev. Lett.* **73**, 34 (1994).

[16] F.M. Marqués, Thèse Université de Valencia (Spain), GANIL T94-05; F.M. Marqués *et al.*, *Phys. Lett.* **B349**, 30 (1995).
[17] F.M. Marqués *et al.*, *Nucl. Instrum. Methods Phys. Res.* **A365**, 392 (1995).
[18] S. Frullani, J. Moguey, *Adv. Nucl. Phys.* **14**, 1 (1985).
[19] G. Martínez *et al.*, *Phys. Lett.* **B334**, 23 (1994).
[20] K. Niita, in II IN2P3 - Riken Symposium on Heavy-Ion Collisions, Obernai, France (1990), eds. B. Heusch and M. Ishihara, World Scientific Publ. Co., 1990, p.342; P. Bożek, M. Płoszajczak, in Gamma Ray and Particle Production in Heavy Ion Reaction, Proc. II TAPS Workshop, Guardamar, Spain (1993), eds J. Díaz, G. Martínez and Y. Schutz, World Scientific Publ. Co., 1994, p.559; M. Belkacem *et al.*, *Phys. Rev.* **C47**, 47 (1993).